Transforming Waste Fish Bones to Nanoparticles with Ultrasound and Aqueous Organic Acids

Sarah Boudreau,[a] Sabahudin Hrapovic,[b] Emma MacIsaac,[a] Edmond Lam,[c] Fabrice Berrué,*[d] and Francesca M. Kerton*[a]

Nano-hydroxyapatite particles were prepared from Atlantic salmon bones using ultrasound in combination with heat, ball-milling and acid treatment. The smallest particles (d = 29 nm) were produced using aqueous propanoic acid and 15 min ultrasound exposure, whereas heat pre-treatment and ultrasound for 60 min led to more well-defined, spherical particles.

As climate change continues to be fuelled by anthropogenic CO_2 emissions, biomass feedstocks have gained significant attention to replace fossil fuels and assist in achievement of net zero goals.[1] Biomass by-products from several industries, such as pulp[2] and agriculture[3], are often wasted. However, they have the potential to be useful for other applications and help in the journey towards a circular economy.[4] For example, there has been much research into repurposing lignin[5,6,7] and cellulose[8,9,10] from plant waste, as well as smaller molecules derived from them.[11,12] While most research in literature focuses on these organic-containing wastes, our group has looked at accessing inorganic materials and minerals from biomass, specifically seafood processing by-products. For example, we have isolated calcium carbonate from waste blue mussel (*Mytilus edulis*) shells[13] and subsequently transformed the shells to a biogenic sponge-like material for the absorption of crude oil and dyes.[14] Recently, our group has optimized an enzymatic method to isolate hydroxyapatite (HAP) from Atlantic salmon (*Salmo salar*) bones[15] and have since been exploring potential applications for this material.

Throughout the last century, nanomaterials[16] have become highly important for biomedicine,[17,18] food processing and packaging,[19] energy storage,[20] environmental remediation,[21,22]

agriculture,[23] catalysis[24] and more.[25] As the number of potential applications continues to increase, there is a need to develop sustainable processes to synthesize nanoparticles. Current methods to synthesize nanoparticles typically involve bottom-up processes, such as sol-gel reactions, chemical vapour deposition, or chemical reduction.[26] These processes often rely on mined or petroleum-derived feedstocks, generate waste and can use hazardous chemicals. That being said, the principles of Green Chemistry can be applied to overcome these obstacles.[27] An emerging green and sustainable technique to synthesize nanoparticles is mechanochemistry.[28] For example, ball-milling has been used for the synthesis of gold[29] and zinc oxide nanoparticles,[30] processes that typically rely on chemical methods.[31,32]

Mechanochemistry has also been explored as a top-down method to yield nanoparticles from biomass.[33] For example, Jin *et al.* have synthesized chitin and chitosan nanocrystals from green crab (*Carcinus maenas*) shells and soft wood pulp, respectively, using a combination of mechanochemistry and aging.[34] Colloidal and stable nanocellulose materials were prepared by Douard *et al.* from ball-milling cotton fibres in deep eutectic solvents.[35] Other organic bio-derived nanomaterials that have been investigated were based on starch, pectin, gum, and alginate.[36] However, there remains a lack of research regarding the transformation of inorganic biomass to nanoparticles using methods based on Green Chemistry. While nano-hydroxyapatite (nHAP) has been prepared previously by Sharifianjazi *et al.* from pigeon (*Columba livia*) bone, the described process relies on high temperatures such as 850 °C before milling.[37] In this study, we have successfully demonstrated that nHAP can be synthesized from Atlantic salmon bones without using large energy expenditures. Ball-milling and sonication, two mechanochemical methods, were

a. Department of Chemistry, Memorial University of Newfoundland, St. John's, NL, Canada. Email: fkerton@mun.ca

b. Aquatic and Crop Resource Development, National Research Council Canada, Montreal, QC, Canada.

c. Department of Chemistry, McGill University, Montreal, QC, Canada.

d. Aquatic and Crop Resource Development, National Research Council Canada, Halifax, NS, Canada. Email: fabrice.berrue@nrc-cnrc.gc.ca

† Electronic Supplementary Information (ESI) available: materials, ultrasound procedure, characterization information, TEM images, DLS, and LCA data.
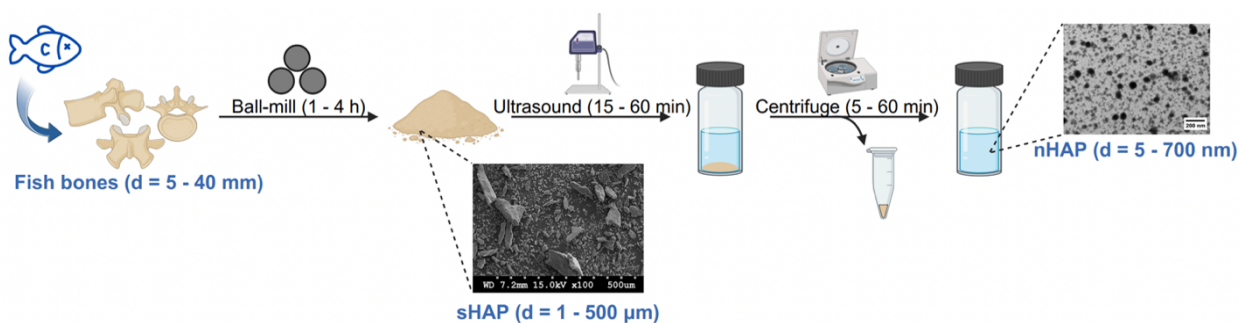
Figure 1. Milling and sonication steps to transform Atlantic salmon bones to nHAP.

used in combination to yield nHAP with tailored size and particle definition.

Waste Atlantic salmon bones were cleaned following our previously reported method.[15] Briefly, salmon frames (backbones) were manually cleaned of excess meat, blended for 1 min, boiled for 1 h in tap water, and enzymatically treated with 15 µL g^{-1} Neutrase and 7.5 µL g^{-1} Lipozyme CALB L for 6 h in water at 40 °C. The bones, referred to as sHAP herein, were allowed to dry in air overnight before being pulverized in a ball-mill for 1 – 4 h with cooling breaks after every 20 min to prevent overheating (see ESI).† A portion of salmon bones were put in an oven for 24 h at 200 °C prior to milling to study the effects of this heat on nanoparticle synthesis.

Samples subjected to ultrasound were treated by dispersing 10 mg sHAP in 10 mL of selected media (e.g., water, aqueous organic acids), Figure 1. The solution was sonicated for 15 – 60 min and centrifuged for 5 – 60 min at 6,000 rpm. The supernatant was decanted and kept for TEM and DLS analyses while the residual pellet was discarded. Characterization of the materials in the residual pellet will be the focus of future research. More details about the experimental setup are found in ESI.† Throughout these studies, experiments were repeated to ensure reproducibility in terms of particle size across a specific set of conditions.

The time period for ball-milling and centrifuging were varied, and their impacts on the average size and distribution of nHAP particles evaluated. For ball-milling, fish bones were ground for 1, 2, 3, and 4 h, and 10 mg of the resulting sHAP powder dispersed in 10 mL water. Dynamic Light Scattering, DLS, data (Table S1) and TEM (Figure S1) confirmed that increased milling time did not have an impact on particle size, and therefore 1 h was chosen for further experiments. The centrifugation time was selected to be 15 min as increased time did not impact particle size and distribution (Table S2).

The choice of sonicating medium was the most important variable affecting the size and uniformity of nHAP particles. Deionized (DI) water, 5% (v/v) propanoic acid (PA), 5% (v/v) acetic acid (AA), and 5% (w/v) oleic acid (OA) were investigated as media by comparing the DLS data and TEM images of resulting particles. nHAP particles synthesized with OA had a significantly higher average particle size of 19,950 nm according to DLS (Table 1) and non-uniformity was observed by TEM (Figure S2), therefore it was not investigated further. Water, 5% PA, and 5% AA yielded spherical nanoparticles that were compared by size distribution histograms (Figure 2) –

throughout this communication size represents the diameter of particles from TEM data, which were analyzed using ImageJ software. While water produced the lowest average particle size (Figure 2 **a,b**), the histogram also had large error bars, especially in the 6 – 10 and >100 nm ranges, possibly from the tendency of water-based nHAP to agglomerate. 5% acetic acid resulted in lower agglomeration; however, most nanoparticles were >100 nm (Figure 2 **c,d**). 5% PA was chosen for further investigation because the resulting nHAP particles were colloidal and smallest based on TEM (Figure 2 **e,f**) and DLS analyses (Table 1).

Table 1. Size, PDI,[a] and zeta-potential of nHAP particles prepared by sonicating 10 mg sHAP in 10 mL water or 5% organic acid for 15 min.[b]

Entry	Medium	Size (nm)	SD[a]	PDI[a]	SD[a]	Zeta (mV)	SD[a]
1	5% OA	19,950	6,181	0.354	0.247	-16.3	5.98
2	Water	677.60	108.4	0.557	0.0840	5.62	0.755
3	5% AA	345.70	3.889	0.546	0.885	16.3	0.985
4	5% PA	252.60	38.70	0.545	0.043	15.2	0.686

a. Abbreviations – standard deviation, SD; polydispersity index, PDI; oleic acid, OA; acetic acid, AA; propanoic acid, PA.
b. Prior to analysis, the sample was centrifuged for 15 min at 6,000 rpm with the supernatant decanted for analysis and the pellet discarded.
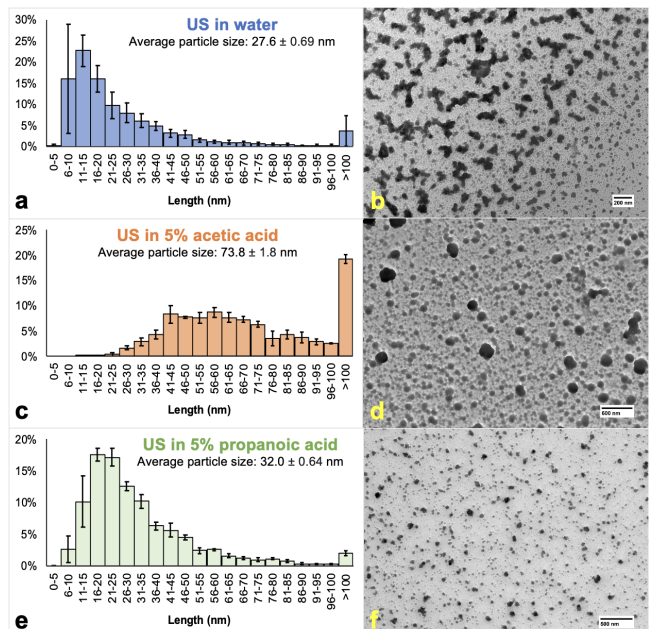
Figure 2. Size distributions and TEM images nHAP samples prepared by ultrasound (US) in water or 5% organic acid for 15 min. Sample a,b (entry 2, top, blue, scale bar: 200 nm, Figure S3) was sonicated in water, c,d (entry 3, middle, orange, scale bar: 600 nm, Figure S4) in 5% AA, and e,f (entry 4, bottom, green, scale bar: 500 nm, Figure S5) in 5% PA. Prior to analysis, the sample was centrifuged for 15 min at 6,000 rpm with the supernatant decanted for analysis and the pellet discarded. Reported diameters are labelled as "length".
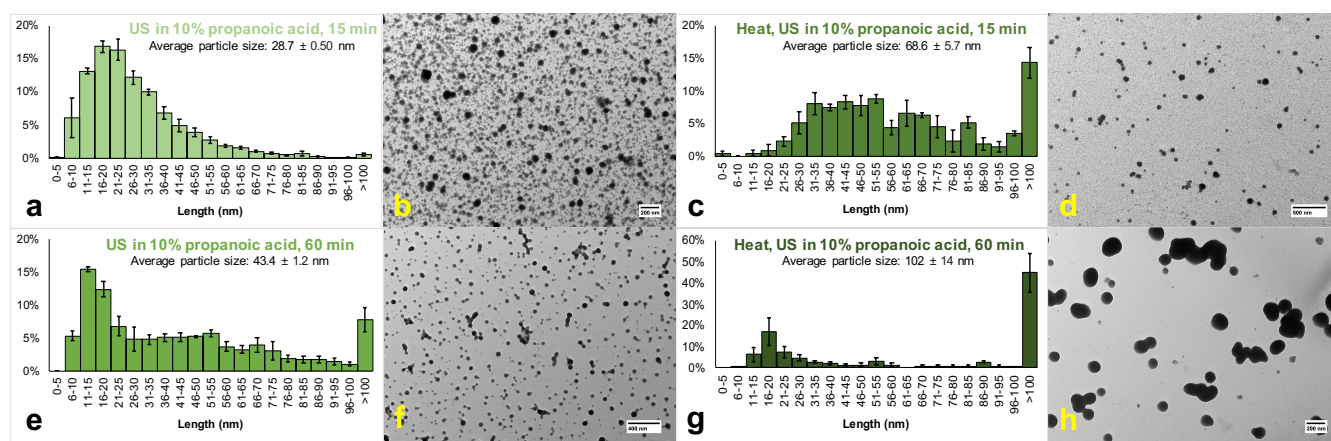
2

Figure 3. Size distribution histograms and TEM images of nHAP samples prepared by ultrasonication (US) in 10% propanoic acid. Samples a,b (top left, Figure S6, scale bar: 200 nm) and c,d (top right, Figure S7, scale bar: 500 nm) were sonicated for 15 min while samples e,f (bottom left, scale bar: 400 nm, Figure S8) and g,h (bottom right, scale bar: 200 nm, Figure S9) were sonicated for 60 min. Samples c,d (top right, scale bar: 500 nm) and g,h (bottom right, scale bar: 200 nm) were pre-treated by placing sHAP into an oven for 24 h at 200 °C before milling. Prior to analysis, the sample was centrifuged for 15 min at 6,000 rpm with the supernatant decanted for analysis and the pellet discarded.

Next, the concentration of PA was increased from 5 to 10% (Figure 3). nHAP particles sonicated in 10% PA for 15 min had more defined edges compared to those produced using 5% PA. We hypothesize that this results from residual collagen within sHAP being decomposed by the higher concentration of acid. Collagen does not conduct electrons and therefore causes a charge build-up during TEM analysis, distorting the image and making observed particles less resolved. Furthermore, the size distribution histogram of nHAP in 10% propanoic acid had a slightly lower average particle size and only 0.5% of particles were larger than 100 nm. Therefore, 10% PA was used herein for further experiments.

Using 10% PA, the sonicating time was increased from 15 to 60 min. Interestingly, while the edges of particles were even more defined (Figure 3 **f**), the average particle size increased significantly from 28.7 ± 0.50 (Figure 3 **a**) to 43.4 ± 1.2 nm (Figure 3 **e**). Although 7.7% of nHAP particles had diameters greater than 100 nm, the reported polydispersity index, PDI, from DLS data was decreased slightly from 0.443 to 0.389 (Table S3).

Increased diameters and PDIs were obtained when sHAP was heated for 24 h at 200 °C before milling. For example, heated samples sonicated for 15 min had a larger average particle size (Figure 3 **c**) than sonicating unheated sHAP for 60 min (Figure 3 **e**). Also, sonicating heated sHAP for 60 min yielded particles with an average particle size of 102 ± 14 nm (Figure 3 **g**) with 45% of particles being greater than 100 nm, and a PDI of 0.837 (Table S3). Collectively, these experiments show that heat, dilute acid used, and ultrasound treatment time period all affect the size and PDI of nHAP produced.

To validate the increased sustainability of our process compared to others reported in literature, we have performed a simplified gate-to-gate life cycle assessment (LCA) for several nHAP procedures, Table 2.[38] This LCA is based on the transformation of fish waste to nHAP without considering the manufacture of additional chemicals used (e.g., PA). More details regarding LCA calculations can be found in the ESI.[†] Our method that relies on ultrasound was compared with processes that have used calcination and/or alkaline deproteinization. Yamamura et al., Biazar et al., and Venkatesan et al. use NaOH

to dissolve the protein residues[39,40,41] and therefore possess significant human ingestion potentials. While Sharifianjazi et al.'s reported method is not hazardous for human exposure because of the lack of chemicals required, it relies on temperatures up to 850 °C to produce nHAP,[37] resulting in a high global warming potential from increased CO_2 emissions.

Table 2. Hot spot analysis of five processes to synthesize nHAP from waste using LCA.[a]

Route	I_{SF}[a]	I_{GW}[a]	I_{INHT}[a]	I_{INGT}[a]	PER[a]
Our method	0	138	0	0	NO
Sharifianjazi et al.[37]	0	4.28×10^3	0	0	NO
Yamamura et al.[39]	0	5.49×10^3	0	3.39×10^5	NO
Biazar et al.[40]	1.81	6.90×10^3	7.17	1.70×10^4	NO
Venkatesan et al.[41]	1.42	901	563	5.17×10^4	MOD

a. Abbreviations – Life Cycle Assessment, LCA; I_{SF}, smog formation potential; I_{GW}, global warming potential; I_{INHT}, human inhalation toxicity potential; I_{INGT}, human ingestion toxicity potential; PER, persistence potential.

In conclusion, we have successfully transformed fish processing industry discards into nHAP particles using environmentally benign conditions. The size and definition of particles can be tailored by heating the bones before sonication, modifying the ultrasound medium and changing the time period of sonication. Higher concentrations of organic acid and heat lead to larger particle sizes, but more defined particles. Larger or smaller particles (30 nm *vs.* 100 nm) can therefore be prepared depending on their desired application. For example, while smaller particles containing collagen could be useful for biomedicine, larger particles have the potential to be explored for new materials applications. Furthermore, our LCA demonstrates a 97% reduction in CO_2 emissions compared with traditional calcination routes.[37] We are now performing studies to understand the nature of the sHAP remaining in the pellet formed upon centrifugation and uses for the nHAP.

Conceptualization, F. M. K; methodology, S. B., E. M., and F. M. K; characterization, S. B. and S. H.; writing – original draft preparation, S. B.; writing – review and editing, S. B., S. H., F. M.

K., and F. B.; supervision, F. M. K. and F. B., funding acquisition, F. M. K. and F. B. All authors listed have agreed to the final version of this communication and have made significant contributions.

Conflicts of interest

There are no conflicts to declare.

Data availability

The data supporting this article have been included as part of the Electronic Supplementary Information.

References

1   United Nations, Climate Change, https://www.un.org/en/global-issues/climate-change, (accessed July 15, 2024).

2   A. Haile, G. G. Gelebo, T. Tesfaye, W. Mengie, M. A. Mebrate, A. Abuhay and D. Y. Limeneh, *Bioresour. Bioprocess.*, 2021, **8**, 35.

3   S. Babu, S. Singh Rathore, R. Singh, S. Kumar, V. K. Singh, S. K. Yadav, V. Yadav, R. Raj, D. Yadav, K. Shekhawat and O. Ali Wani, *Bioresour. Technol.*, 2022, **360**, 127566.

4   J. H. Clark, T. J. Farmer, L. Herrero-Davila and J. Sherwood, *Green Chem.*, 2016, **18**, 3914–3934.

5   B. L. Tardy, E. Lizundia, C. Guizani, M. Hakkarainen and M. H. Sipponen, *Mater. Today*, 2023, **65**, 122–132.

6   M. J. Gan, Y. Q. Niu, X. J. Qu and C. H. Zhou, *Green Chem.*, 2022, **24**, 7705–7750.

7   C. Zhang, X. Shen, Y. Jin, J. Cheng, C. Cai and F. Wang, *Chem. Rev.*, 2023, **123**, 4510–4601.

8   F. D'Acierno, C. A. Michal and M. J. MacLachlan, *Chem. Rev.*, 2023, **123**, 7295–7325.

9   Y. Ai, L. Zhang, M. Cui, R. Huang, W. Qi, Z. He, J. J. Klemeš and R. Su, *Green Chem.*, 2022, **24**, 6406–6434.

10 M. Gao, Y. Shang, B. Li and H. Du, *Green Chem.*, 2022, **24**, 9346–9372.

11 R. Hu, J. Zhan, Y. Zhao, X. Xu, G. Luo, J. Fan, J. H. Clark and S. Zhang, *Green Chem.*, 2023, **25**, 8970–9000.

12 A. Kumar, A. Singh Chauhan, R. Bains and P. Das, *Green Chem.*, 2023, **25**, 849–870.

13 J. N. Murphy, K. Hawboldt and F. M. Kerton, *Green Chem.*, 2018, **20**, 2913–2920.

14 J. N. Murphy, C. M. Schneider, K. Hawboldt and F. M. Kerton, *Matter*, 2020, **3**, 2029–2041.

15 S. Boudreau, S. Hrapovic, Y. Liu, A. C. W. Leung, E. Lam and F. M. Kerton, *RSC Sustain.*, 2023, **1**, 1554–1564.

16 M. Österberg, K. A. Henn, M. Farooq and J. J. Valle-Delgado, *Chem. Rev.*, 2023, **123**, 2200–2241.

17 J. Zhao and M. H. Stenzel, *Polym. Chem.*, 2018, **9**, 259–272.

18 F. Fang, M. Li, J. Zhang and C.-S. Lee, *ACS Materials Lett.*, 2020, **2**, 531–549.

19 J. Chen, Y. Guo, X. Zhang, J. Liu, P. Gong, Z. Su, L. Fan and G. Li, *J. Agric. Food Chem.*, 2023, **71**, 3564–3582.

20 Z. Gan, J. Yin, X. Xu, Y. Cheng and T. Yu, *ACS Nano*, 2022, **16**, 5131–5152.

21 H. Rafeeq, A. Hussain, A. Ambreen, Zill-e-Huma, M. Waqas, M. Bilal and H. M. N. Iqbal, *J. Nanostruct. Chem.*, 2022, **12**, 1007–1031.

22 R. Das, T. Lindström, P. R. Sharma, K. Chi and B. S. Hsiao, *Chem. Rev.*, 2022, **122**, 8936–9031.

23 R. Saberi Riseh, M. Hassanisaadi, M. Vatankhah, R. S. Varma and V. K. Thakur, *Nano-Micro Lett.*, 2024, **16**, 147.

24 A. Srivastava, H. Kaur, H. Pahuja, T. M. Rangarajan, R. S. Varma and S. Pasricha, *Coord. Chem. Rev.*, 2024, **507**, 215763.

25 B. Thomas, M. C. Raj, A. K. B, R. M. H, J. Joy, A. Moores, G. L. Drisko and C. Sanchez, *Chem. Rev.*, 2018, **118**, 11575–11625.

26 N. Baig, I. Kammakakam and W. Falath, *Mater. Adv.*, 2021, **2**, 1821–1871.

27 M. Lancaster, *Green Chemistry 3rd Edition: An Introductory Text*, Royal Society of Chemistry, 2016.

28 B. G. Fiss, A. J. Richard, G. Douglas, M. Kojic, T. Friščić and A. Moores, *Chem. Soc. Rev.*, 2021, **50**, 8279–8318.

29 A. J. Richard, M. Ferguson, B. G. Fiss, H. M. Titi, J. Valdez, N. Provatas, T. Friščić and A. Moores, *Nanoscale Adv.*, 2023, **5**, 2776–2784.

30 S. Wirunchit, P. Gansa and W. Koetniyom, *Mater. Today: Proceedings*, 2021, **47**, 3554–3559.

31 P. Suchomel, L. Kvitek, R. Prucek, A. Panacek, A. Halder, S. Vajda and R. Zboril, *Sci. Rep.*, 2018, **8**, 4589.

32 Th. A. Singh, J. Das and P. C. Sil, *Adv. Colloid Interface Sci.*, 2020, **286**, 102317.

33 F. Hajiali, T. Jin, G. Yang, M. Santos, E. Lam and A. Moores, *ChemSusChem*, 2022, **15**, e202102535.

34 T. Jin, T. Liu, F. Hajiali, M. Santos, Y. Liu, D. Kurdyla, S. Régnier, S. Hrapovic, E. Lam and A. Moores, *Angew. Chem. Int. Ed.*, 2022, **61**, e202207206.

35 L. Douard, M. N. Belgacem and J. Bras, *ACS Sustain. Chem. Eng.*, 2022, **10**, 13017–13025.

36 M. Nasrollahzadeh, M. Sajjadi, S. Iravani and R. S. Varma, *Carbohydr. Polym.*, 2021, **251**, 116986.

37 F. Sharifianjazi, A. Esmaeilkhanian, M. Moradi, A. Pakseresht, M. S. Asl, H. Karimi-Maleh, H. W. Jang, M. Shokouhimehr and R. S. Varma, *Materials Science and Engineering: B*, 2021, **264**, 114950.

38 S. M. Mercer, J. Andraos and P. G. Jessop, *J. Chem. Educ.*, 2012, **89**, 215–220.

39 H. Yamamura, V. H. P. da Silva, P. L. M. Ruiz, V. Ussui, D. R. R. Lazar, A. C. M. Renno and D. A. Ribeiro, *J. Mech. Behav. Biomed. Mater.*, 2018, **80**, 137–142.

40 E. Biazar, M. Daliri J, S. Heidari K, D. Navayee A, M. Kamalvand, M. Sahebalzamani, F. Royanian, M. Shabankhah and F. Farajpour L, *J. Bioeng. Res.*, 2020, **2**, 10–19.

41 J. Venkatesan, B. Lowe, P. Manivasagan, K.-H. Kang, E. P. Chalisserry, S. Anil, D. G. Kim and S.-K. Kim, *Mater. (Basel)*, 2015, **8**, 5426–5439.

Table of Contents Image & Accompanying Text

Salmon by-product streams can yield hydroxyapatite nanoparticles using green and sustainable methods. Clean bones were ball-milled and treated with ultrasound to give spherical nanoparticles (diameters < 100 nm).